King's Research Portal

Modular supramolecular dimerization of optically-tunable extended aryl viologens[†]

Magdalena Olesińska,[a] Guanglu Wu,[a] Silvia Gómez-Coca,[b] Daniel Antón-García,[c] Istvan Szabo,[b] Edina Rosta,[b] and Oren A. Scherman[*a]

Cucurbit[8]uril (CB[8]) mediated assembly of extended aryl viologens (EVs) into optically-tunable dimers is reported for the first time. We show that modular design and synthesis of a new class of π-conjugated viologen derivatives with rigid aromatic or heteroaromatic bridging units as well as electron donating molecular recognition motifs enables their self-assembly into 2:2 complexes with CB[8]. The quantitative dimerization process involving these two molecular components in an aqueous solution enables excimer-like interactions between closely packed charged guests giving rise to distinct spectroscopic behavior. The nature of these dimers $\left(\mathrm{CB}[8]_2 \cdot (\mathrm{EV}[\mathrm{X}]\mathrm{R})_2\right)$ in the ground and excited states were characterized by NMR, isothermal titration calorimetry, and steady-state spectroscopic measurements

Achieving precise control over the spatial arrangement of organic photoemissive molecules is of interest in the area of photovoltaic device construction, light-emitting diodes[1], sensing and bio-imaging.[2] Both covalent and non-covalent interactions between fluorescent molecules have been used in order to optimize their best optical properties. Recently, a number of examples have been reported in the literature, which detail control over the emissive states of discrete organic molecules or complexes including luminescence of molecular rotors based on aggregation induced emission[3], generation of excimers with modifications in covalently-bound chromophores[4–6] and H- and J-aggregate formation on account of encapsulation within supramolecular macrocycles or self-assembled cages.[7–16] Nevertheless, these sys-

tems are synthetically challenging and do not provide a modular approach for tuning optoelectronic properties.

Cucurbit[n]urils (CB[n]) are a family of macrocyclic host molecules often used in synthetic and material sciences on account of their variety of sizes and capability to complex different types of guest molecules in an aqueous environment.[17] In particular, cucurbit[8]uril (CB[8]) is of interest due to its abil-
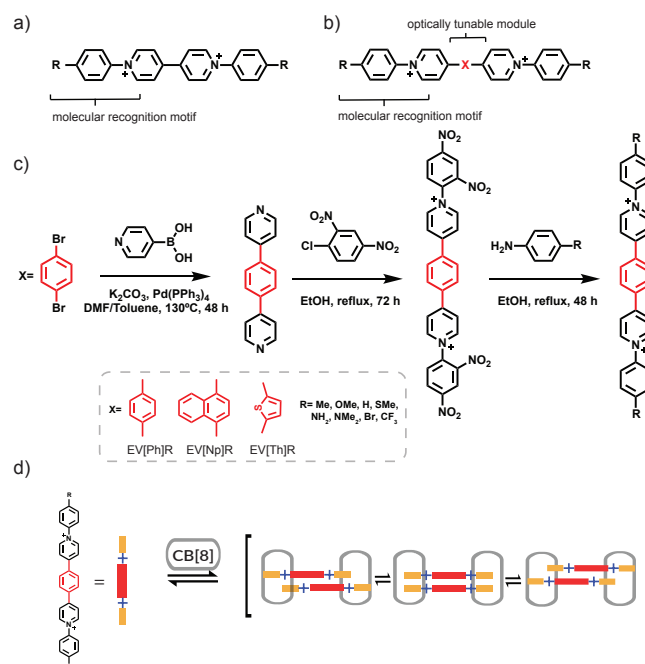
Fig. 1 a) Aryl viologen used in previous work with molecular recognition motif (Ph-R) for CB[8] binding. b) The extended aryl viologen design principle, with optical tunable (X) and molecular recognition (Ph-R) modules used in this work. c) General synthetic route towards extended aryl viologens (EVs). d) Scheme of 2:2 $\mathrm{CB}[8]_2 \cdot (\mathrm{EV}[\mathrm{Ph}]\mathrm{R})_2$ complex formation for R groups with electron donating character. The Cl$^-$ counterions have been omitted for clarity.

[a] *Melville Laboratory for Polymer Synthesis, Department of Chemistry, University of Cambridge, Lensfield Road, Cambridge, CB2 1EW, UK. E-mail: oas23@cam.ac.uk*
[b] *Department of Chemistry, King's College London, 7 Trinity Street, London, SE1 1DB, UK.*
[c] *Department of Chemistry, University of Cambridge, Lensfield Road, Cambridge CB2 1EW, UK.*

ity to host two guest moieties simultaneously. We previously described the binding of CB[8] with symmetric diaryl viologens bearing electron-donating groups (Fig.1a) in a 2:2 binding fashion, representing an understudied binding mode in the literature.[18]. The formation of such 2:2 complexes led to interesting changes of their optical properties. We observed a uniform red-shift in the absorption of the 2:2 complexes relative to their monomeric UV/Vis spectra, and in a few specific cases (R= Me or OMe) an intense fluorescence emission typical for J-aggregates (see Figure S75).[18] Similar observation of enhanced photoluminescence for 2:2 complexes of CB[8] and viologen derivatives were recently described.[19,20]

In order to take advantage of strict 2:2 complex formation through the CB[8] binding motif we explored the introduction of an extended π-bridging unit between the two pyridyl groups as shown in Figure 1b. Symmetric extended aryl viologen (EV) derivatives with various conjugated cores *i.e.* phenyl (EV[Ph]), naphthyl (EV[Np]) and thiophene (EV[Th]) were synthesized in a three-step procedure, as depicted in Figure 1c. Bipyridine derivatives were made through Suzuki coupling of pyridine 4-boronic acid and the corresponding dibromo species. These bipyridine derivatives were then subjected to a two-step Zinke reaction with formation and isolation of the symmetric Zinke salt. Subsequent reaction of the symmetric Zinke salt with appropriate amines yielded the various extended aryl viologens, EV[Ph]R, EV[Np]R and EV[Th]R (see ESI). The directing capability of the CB[8] macrocycle around the aryl pyridyl groups facilitate π - π stacking of the linker units and control the spatial arrangement of the EV monomers. The donor-acceptor character of molecules coupled in close proximity imposed by CB[8] macrocycles leads to positive or negative Coulombic interaction.[21] This results in competition between a favorable electrostatic interaction as well as π-π stacking that has a strong effect on photophysical performance of the formed dimers.[22]

We report here the extent of inter-chromophoric interactions in the ground and excited states based on their steady-state electronic transitions and fluorescence lifetimes as a function of their binding with CB[8]. We hypothesized that the emissive excited state properties of the dimeric complexes $CB[8]_2 \cdot (EV[X]R)_2$ would not only be influenced by the host-guest interactions in their ground state but also in their excited state as an excimer-like complex. Previous observations have been made for molecular packing of naphthalene, anthracene and phenanthrene under pressure or in the solid state with energies of their electronic transitions shifted towards the red (lower energy), and their broadened and featureless spectral bands.[23] In our system, complexation inside the confined space of the CB[8] macrocycles results in distinct π-stacking in solution. It was recently shown that the distance between molecules affects charge transfer interactions and excimer formation.[4]. However, the recent report by Wu *et al.* and many other reports are focused mostly on covalent dimers where the dimeric units are not free to rotate or rearrange.[2,4,24–26] Given that the supramolecular dimeric systems reported here are dynamic, we reasoned that upon excitation, the two guest molecules are still able to rearrange in their excited states within the complex and reach the most stable excited state
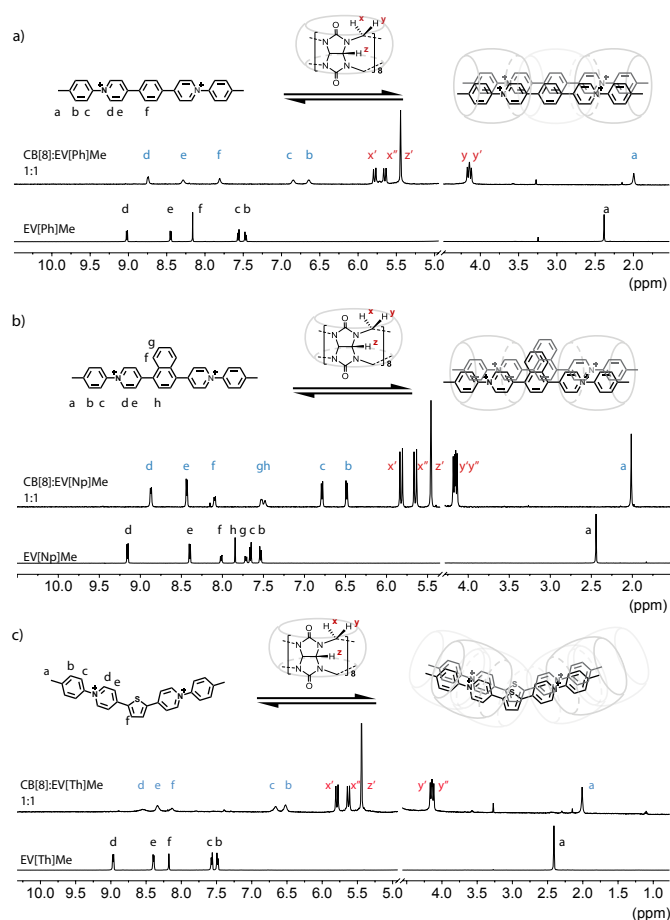
geometry.

Fig. 2 ^1H NMR spectra ($500\,\mathrm{MHz}$) of (a) EV[Ph]Me, (b) EV[Np]Me, (c) EV[Th]Me and their complexes with 1 eq of CB[8] (D_2O, $298\,\mathrm{K}$). The Cl$^-$ counterions have been omitted for clarity.

Following synthesis and characterization, the binding properties of these new extended aryl viologens with CB[8] were probed using spectroscopic and thermodynamic techniques, including ^1H NMR and isothermal titration calorimetry (ITC). Typical NMR experiments are carried out at 100 uM at room temperature where the 2:2 complexes form instantly. Guest complexation with the hydrophobic cavity of CB[8] typically results in an upfield shift of the encapsulated protons and a downfield shift of protons in close proximity to the carbonyl portals as shown in Figure 2. Interestingly, titration of EV[Ph]Me into a solution of CB[8] led to a broadening of the guest signals (Figure 2a and Figure S52). The proton integration ratio of EV[Ph]Me mixed with CB[8] suggests the formation of a dynamic 2:2 host-guest complex (See ESI Figure S49). The broad NMR peaks are attributed to the unencumbered aromatic linker unit, in this case a phenyl ring, which is small enough to allow the CB[8] macrocycles to shuttle back and forth in the 2:2 complex. Augmenting the bridging unit from Ph to Np results in a complex that appears to be less dynamic as the bulkier Np dimer retards the rate of CB shuttling. Upon titration of the bulkier EV[Np]Me molecule into a

CB[8] solution, a 0.5 ppm upfield shift of methyl proton H_a was observed (Figure 2b and Figure S56) at a 1:1 ratio, indicative of encapsulation or partial encapsulation inside the cavity of CB[8]. Incorporation of a heteroatom in the bridging species was also possible resulting in an extended viologen bearing a thiophene unit, EV[Th]Me. Analogous proton shifts of the tolyl group and thiophene core were observed (Figure 2c and Figure S67) upon 2:2 complex formation with EV[Th]Me; a pronounced broadening of peaks in the CB[8]:EV[Th]Me complex suggests an increase of dynamics in such a system.

Regardless of bridging unit, all of the EVs studied revealed a 2:2 binding motif, which could be confirmed from the unique splitting pattern of peaks in the NMR corresponding to the asymmetric magnetic field for methine protons at the CB[8] portals.[18] The size and geometric orientation of the aromatic bridging unit, however, may have an effect on shuttling dynamics and relative location of the CB[8] macrocycle in the complex. Moreover, bridging units with a larger aromatic surface area, such as naphthalene, lead to a less dynamic complex, that may benefit from stronger $\pi - \pi$ interactions.

The EV-CB[8] complexes were further evaluated using ITC. Our recent work showed that formation of CB[8] complexes is readily characterized by the magnitude of the overall binding enthalpy (ΔH), typically around $-70\,\mathrm{kJ\,mol^{-1}}$.[18] Enthalpy data obtained for all the EVs bearing electron donating groups were found to range from $-90\,\mathrm{kJ\,mol^{-1}}$ to $-70\,\mathrm{kJ\,mol^{-1}}$ suggesting 2:2 binding with CB[8] (see ESI) in agreement with ^1H NMR (Figure 2). Additionally, the binding constants (K_a) for the EV and CB[8] complexes were found to be within $5.5 \times 10^6\,\mathrm{M^{-1}}$ to $3.8 \times 10^7\,\mathrm{M^{-1}}$, indicating strong host-guest binding. Importantly, when EV[Np]R bearing electron withdrawing groups (R= CF$_3$ and Br) were mixed with a stoichiometric amount of CB[8], the complexes formed were not found to bind in a 2:2 manner, but rather yielded 1:1 or n:n complexes confirmed by NMR and ITC measurements (see ESI).

Complexation inside the CB[8] cavity affects the local environment of extended viologens, which in turn alters their optical properties. It has been reported that encapsulation in CB[8] causes a red shift in the absorption and emission bands, as well as an increase in the fluorescence quantum yield (Φ_{PL}) and fluorescence lifetime (τ).[10,27–30] For the extended viologens reported here, we expect the structural differences within this series (increasing the π-surface area and inclusion of a heteroaromatic in the bridging unit) to augment both complexation with CB[8] as well as their respective electronic transition energies. Normalized steady-state absorption and emission spectra of the three EVs studied in the absence and presence of 1 eq of CB[8] are shown in Figure 3. The spectral properties are summarized in Table 1.

UV/Vis and emission spectra of all three EV[X]Me reveal a red shift in the absorption and fluorescence emission upon increasing the aromatic conjugation or incorporating a heteroatom within the core (see Figure 3).

The ground-state UV/Vis absorption spectra of EV[Ph]Me (solid black line, Figure 3a) in water shows a maximum absorption band at $\lambda_{\mathrm{abs}} = 343\,\mathrm{nm}$ ($\varepsilon = 24\,400\,\mathrm{M^{-1}\,cm^{-1}}$) and a broad, featureless emission band with a maximum at $\lambda_{\mathrm{em}} = 456\,\mathrm{nm}$
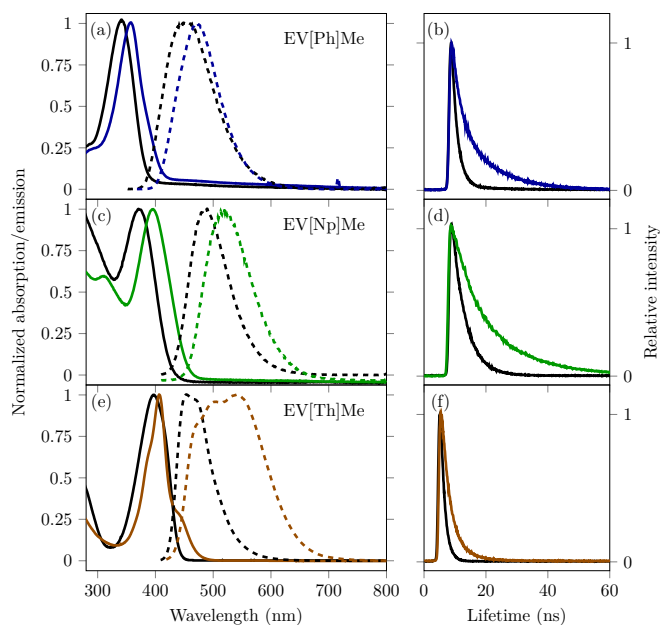

Fig. 3 Left graph: Normalized absorption (solid lines) and fluorescence (dashed lines) spectra of extended viologens (a) EV[Ph]Me, (c) EV[Np]Me, (e) EV[Th]Me (black lines) and their complexes with 1 eq of CB[8] (colored lines); Right graph: Time-correlated single photon counting decay profiles for (b)EV[Ph]Me (black line) and EV[Ph]Me:CB[8] in 2:2 mix (blue line), (d) EV[Np]Me (black line) and EV[Np]Me:CB[8] in 2:2 mix (green line), and (f) EV[Th]Me (black line) and EV[Th]Me:CB[8] in 2:2 mix (orange line). All measurements were performed in water, with the guest concentration of $10\,\mu\mathrm{M}$.

($\Phi_{PL} = 0.65$). Upon mixing with 1 eq of CB[8], bathochromic shifts of over $10\,\mathrm{nm}$ in the absorption and emission spectra are observed, as well as strong enhancement in the fluorescence quantum yield (Φ_{PL}=0.92). Similarly, for EV[Np]Me (solid black line, Figure 3c) the ground-state UV/Vis absorption spectra is characterized by a maximum absorption band at $\lambda_{\mathrm{abs}} = 371\,\mathrm{nm}$ (ε=15 700 $\mathrm{M^{-1}\,cm^{-1}}$) and emission band at $\lambda_{\mathrm{em}} = 487\,\mathrm{nm}$ ($\Phi_{PL} = 0.68$). Upon mixing with 1 eq of CB[8], a $25\,\mathrm{nm}$ red-shift in the absorption and $31\,\mathrm{nm}$ red-shift in the emission spectra are observed, as well as a small decrease in fluorescence quantum yield (Φ_{PL}=0.58). The UV/Vis absorption spectra of EV[Th]Me (solid black line, Figure 3e) in water shows a maximum in the absorption band at $\lambda_{\mathrm{abs}} = 397\,\mathrm{nm}$ ($\varepsilon = 51\,740\,\mathrm{M^{-1}\,cm^{-1}}$) and the maximum in the emission band at $\lambda_{\mathrm{em}} = 453\,\mathrm{nm}$ ($\Phi_{PL} = 0.62$). Upon mixing with 1 eq of CB[8], a $10\,\mathrm{nm}$ red-shift in the absorption and $91\,\mathrm{nm}$ red-shift in the emission spectra are observed.

Unlike the cases of EV[Ph]Me and EV[Np]Me, a huge decrease in fluorescence quantum yield is recorded for EV[Th]Me($\Phi_{PL} = 0.07$). The emission spectrum observed for EV[Th]Me complexed with CB[8] has characteristics of typical excimer-like species; here, where 2:2 complex formation is evident, two thiophene bridging moieties are electronically coupled in the excited state. Correspondingly, monomeric EV[Th]Me and de-aggregated 2:1 complexes with CB[7] have high quantum yields of 0.62 and 0.67, respectively (see ESI). The Stokes shift of $122\,\mathrm{nm}$ ($5947\,\mathrm{cm^{-1}}$) (for the CB[8]$_2 \cdot$(EV[Np]Me)$_2$ and $137\,\mathrm{nm}$ ($6187\,\mathrm{cm^{-1}}$) for the

Table 1 Steady-state spectral data of the EV[X]Me in water.

Guest	Host	λ_{abs}^{max} [nm] (ε [M^{-1} cm^{-1}])^a	λ_{em}^{max} [nm]	Stokes shift [nm] [$\Delta\upsilon$(cm^{-1})]	Φ_{PL}^b	τ_{S1} (ns)^c	k_{rad}^d ($\times10^8$ s^{-1})	k_{nrad}^e ($\times10^8$ s^{-1})
EV[Ph]Me	-	343 (24400)	456	113 (7225)	0.65	1.5	4.33	2.33
EV[Ph]Me	CB[8]	357 (37200)	472	115 (6824)	0.92	2.5 (23%) 10.9(77%)	0.84	0.07
EV[Np]Me	-	371 (15700)	487	116 (6348)	0.68	4.2	1.62	0.76
EV[Np]Me	CB[8]	396 (24900)	518	122 (5947)	0.58	6.8 (31%) 17.1(69%)	0.33	0.24
EV[Th]Me	-	397 (51740)	453	56 (3114)	0.62	1.3	4.77	2.93
EV[Th]Me	CB[8]	407 (77700)	544	137 (6187)	0.07	2.7 (82%) 6.7 (18%)	0.26	3.44

^{a}The molar absorptivities at the wavelength, λ_{abs}^{max}; ^{b}Fluorescence quantum yield at r.t.; ^{c}Fluorescence lifetime; ^{d}Fluorescence radiative rate estimated by the equation $k_{rad} = \Phi_{PL}/\tau_{S1}$; $^e k_{nrad} = (1/\tau_{S1}) - k_{rad}$.

CB[8]$_2 \cdot$ (EV[Th]Me)$_2$ complexes indicate that the dipole moments of the photoexcited states have been changed significantly, suggesting formation of intramolecular charge transfer states. Broad, unstructured red-shifted emission is characteristic of charge-transfer transitions as highlighted by Wasielewski and co-workers.[4] Moreover, these are also characteristic steady-state parameters exhibited by excimers or excimer-like species.

Time-correlated single photon counting (TCSPC) of the EVs alone and in the presence of 1 eq of CB[8] were carried out to gain insight into possible EV-EV interactions and their dynamics in the excited state. Figure 3 highlights the emission decay profiles, and the corresponding lifetime data are detailed in Table 1. Following the excitation of EV[Ph]Me at its λ_{em}^{max}, the major emissive component decays with a time constant of 1.5 ns. Upon encapsulation within the CB[8] cavity, long-lived fluorescence was observed with a decay time of 10.9 ns. Additionally, EV[X]Me with increased π-surface area showed longer fluorescence lifetimes, decaying with a time constant of 17 ns. The long-lived emission of these complexes indicates the existence of a stable, long-lived excited state.

It has been reported that inclusion of dye molecules inside CBs leads to a decrease in k_{nrad} on account of the mechanical protection from quenchers present in solution.[29,31,32] However, the (CB[8]$_2 \cdot$ (EV[X]Me)$_2$) complexes for X= Ph and Np give rise to a notable decrease in both k_{rad} and k_{nrad}. In the case of the (CB[8]$_2 \cdot$ (EV[Th]Me)$_2$) complex we observed lower radiative but higher non-radiative decay rates in comparison to free guests (see Table 1). On one hand such observations could be explained by a high non-radiative decay due to inter-system crossing or internal conversion within this complex. On the other hand the photophysical processes occurring within the 2:2 complex clearly depend on the core structure, molecular geometry, and the way the stacking occurs withing the distinct dimeric complex.[21,33]

To gain more insight into dynamic, static and spectroscopic properties of the EV-CB[8] dimeric complexes, molecular dynamics (MD) simulations were performed, followed by quantum chemical calculations. Molecular interactions in our MD simulations include both Coulombic repulsion and $\pi - \pi$ attraction between the pairs of EVs, leading to the observed dynamic behavior of the complexes (see ESI and simulation movies). The simulations suggest a more dynamic behavior of EV[Ph]Me compared to EV[Np]Me or EV[Th]Me in agreement with experimental observations. The MD structures were used as initial starting points to carry out further quantum chemical calculations. We used a recently developed semiempirical method, GFN-xTB[34] that has been demonstrated to successfully model supramolecular complexes.[35] Furthermore, it can also be combined with the sTDA approximation for calculation of the UV spectra (for details see ESI).[36,37] To explore different aggregates at this level of theory, we first clustered the structures from the MD simulation trajectories and selected representative geometries as starting points for the geometry optimizations. The most stable optimized molecular structures of EV[Ph]Me, EV[Np]Me, and EV[Th]Me complexed with CB[8] in a 2:2 manner using TB-DFT are shown in Figure 4, together with their characteristic geometric parameters in Table S4. In the optimized structures, the CB[8]-complexed guest molecules have short $\pi - \pi$ distances between each other. Furthermore, they also show slightly shorter distances between the parallel rings of the guest molecules. The obtained optimized geometries suggest a stronger effect of $\pi - \pi$ interactions and a smaller Coulombic repulsion giving rise to final structures that stabilized head-to-head geometries compared with head-to-tail arrangements.

The calculated spectroscopic properties of the EVs show good agreement with the experimental absorption spectra, displaying red shifts in absorption upon increasing the aromatic conjugation or incorporation of a heteroatom (see Figure S83). In the case of the EV-CB[8] dimeric complexes, no shift or a small blue shift in the calculated absorption spectra is observed (see Figure S84). This suggests enhanced stability of the H-stacked instead of J-stacked guest dimers in the semiempirical calculations, which is likely due to using implicit solvent in the quantum chemical calculations. Accordingly, MD structures show more balanced interactions with considerably longer intercentroid distances (d_c) and shifts (d_{s1} and d_{s2}) between the rings as compared with the geometry optimized structures (Figure S80-82). The presence of explicit water interacting with both the EVs and CB[8] therefore might play a role in increasing the stability of the J-type orientation.

We have described the synthesis of a new family of extended viologen compounds with increasing π-surfaces between the two pyridinium units. The binding properties of this family of molecules with CB[8] is assessed through ^1H NMR and ITC measurements and all three EVs result in the formation of explicit
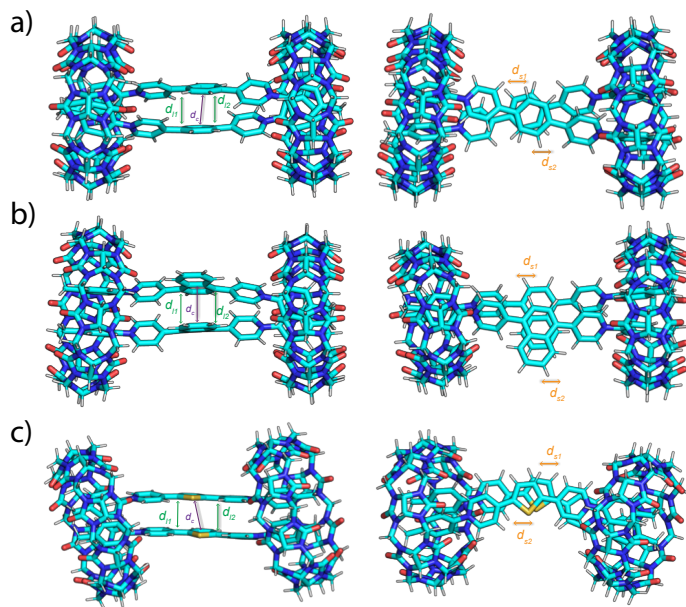
Fig. 4 Front and top view of GFN2-xTB DFT-computed ground-state geometries of 2:2 complexes of CB[8] with a) EV[Ph]Me, b) EV[Np]Me, c) EV[Th]Me. In figure centroid distances (d_c, purple), distances between parallel planes (d_{l1} and d_{l2}, green) and intercentroid shifts (d_{s1} and d_{s2}, orange) between the rings are also indicated by arrows (see ESI).

2:2 host-guest complexes. The optical properties of the resulting supramolecular assemblies were probed and 2:2 assembly in water was found to result in the formation of discrete dimers with tunable luminescence. Two EVs in particular exhibited high absorptivity upon complexation with CB[8] and produce bright blue (EV[Ph]Me) and green (EV[Np]Me) emission, respectively. For these two EVs, the fluorescence spectra exhibited red-shifted, broad, structureless bands with fluorescence quantum yields as high as 0.92 and long fluorescence lifetimes up to 17 ns. On the other hand, EV[Th]Me with a heteroatom in the bridging moiety, resulted in an emission spectrum typical of excimer-like structures with weak orange luminescence. Here in the benzene-naphtalene-thiophene series, stronger $\pi - \pi$ interactions through an increase of aromatic surfaces and, consequently, the restricted rotation or rearrangement in the cavity of CB[8] molecules affect the formation and optical efficiency of excited dimers. Our results suggest that CB[8]-extended aryl viologen supramolecular complexes are a new way to form distinct dimeric entities through a straightforward, synthetically accessible modular approach. These systems represent a platform for studying excited dimers in excited state such as excimers or exciplexes. Furthermore, systematic modification of a bridging unit of extended aryl viologen derivatives will lead to range of systems with long-lived excited states. Finally, on account of such interesting optical properties, these distinct dimers can find myriad applications in imaging.[6]

Conflicts of interest

There are no conflicts to declare.

Acknowledgments

Notes and references

1 Y. Xia, S. Chen and X. L. Ni, *ACS Appl. Mater. Interfaces*, 2018, **10**, 13048–13052.
2 X. Zhang, S. Rehm, M. M. Safont-Sempere and F. Würthner, *Nat. Chem.*, 2009, **1**, 623–629.
3 J. Sturala, M. K. Etherington, A. N. Bismillah, H. F. Higginbotham, W. Trewby, J. A. Aguilar, E. H. Bromley, A. J. Avestro, A. P. Monkman and P. R. McGonigal, *J. Am. Chem. Soc.*, 2017, **139**, 17882–17889.
4 Y. Wu, J. Zhou, B. T. Phelan, C. M. Mauck, J. F. Stoddart, R. M. Young and M. R. Wasielewski, *J. Am. Chem. Soc.*, 2017, **139**, 14265–14276.
5 P. Deria, J. Yu, T. Smith and R. P. Balaraman, *J. Am. Chem. Soc.*, 2017, **139**, 5973–5983.
6 B. Santiago-Gonzalez, A. Monguzzi, J. M. Azpiroz, M. Prato, S. Erratico, M. Campione, R. Lorenzi, J. Pedrini, C. Santambrogio, Y. Torrente, F. De Angelis, F. Meinardi and S. Brovelli, *Science*, 2016, **353**, 571–575.
7 X. L. Ni, S. Chen, Y. Yang and Z. Tao, *J. Am. Chem. Soc.*, 2016, **138**, 6177–6183.
8 M. Yamashina, M. M. Sartin, Y. Sei, M. Akita, S. Takeuchi, T. Tahara and M. Yoshizawa, *J. Am. Chem. Soc.*, 2015, **137**, 9266–9269.
9 N. Barooah, J. Mohanty and A. C. Bhasikuttan, *Chem. Commun.*, 2015, **51**, 13225–13228.
10 H. J. Kim, D. R. Whang, J. Gierschner and S. Y. Park, *Angew. Chem. Int. Ed.*, 2016, **55**, 15915–15919.
11 S. Gadde, E. K. Batchelor, J. P. Weiss, Y. Ling and A. E. Kaifer, *J. Am. Chem. Soc.*, 2008, **130**, 17114–17119.
12 J. Mohanty, S. D. Choudhury, H. P. Upadhyaya, A. C. Bhasikuttan and H. Pal, *Chem. Eur. J.*, 2009, **15**, 5215–5219.
13 A. Ueno, K. Takahashi and T. Osa, *J. Chem. Soc. Chem. Commun.*, 1980, 921–922.
14 A. Ueno, F. Moriwaki, T. Osa, F. Hamada and K. Murai, *J. Am. Chem. Soc.*, 1988, **110**, 4323–4328.
15 A. Ueno, I. Suzuki and T. Osa, *Anal. Chem.*, 1990, **62**, 2461–2466.
16 S. R. McAlpine and M. A. Garcia-Garibay, *J. Am. Chem. Soc.*, 1998, **120**, 4269–4275.
17 S. J. Barrow, S. Kasera, M. J. Rowland, J. Del Barrio and O. A. Scherman, *Chem. Rev.*, 2015, **115**, 12320–12406.
18 G. Wu, M. Olesińska, Y. Wu, D. Matak-Vinkovic and O. A. Scherman, *J. Am. Chem. Soc.*, 2017, **139**, 3202–3208.
19 S. Schoder, H. V. Schröder, L. Cera, R. Puttreddy, A. Güttler, U. Resch-Genger, K. Rissanen and C. A. Schalley, *Chem. Eur. J.*, 2019, **25**, 3257–3261.
20 B. Zhang, Y. Dong, J. Li, Y. Yu, C. Li and L. Cao, *Chin. J. Chem.*, 2019, **37**, 269–275.
21 C. Zheng, C. Zhong, C. J. Collison and F. C. Spano, *J. Phys. Chem. C*, 2019, acs.jpcc.8b11416.
22 L. Shi, Y. Duan, X. Yang and L. Qin, *Comput. Mater. Sci.*, 2010, **49**, 524–529.
23 P. F. Jones and M. Nicol, *J. Chem. Phys.*, 1968, **48**, 5440–5447.
24 O. Khorev, C. D. Bösch, M. Probst and R. Häner, *Chem. Sci.*, 2014, **5**, 1506–1512.
25 R. E. Cook, B. T. Phelan, R. J. Kamire, M. B. Majewski, R. M. Young and M. R. Wasielewski, *J. Phys. Chem. A*, 2017, **121**, 1607–1615.
26 K. E. Brown, W. A. Salamant, L. E. Shoer, R. M. Young and M. R. Wasielewski, *J. Phys. Chem. Lett.*, 2014, **5**, 2588–2593.
27 X. L. Ni, X. Xiao, H. Cong, Q. J. Zhu, S. F. Xue and Z. Tao, *Acc. Chem. Res.*, 2014, **47**, 1386–1395.
28 R. Ye, Q. Cui, C. Yao, R. Liu and L. Li, *Phys. Chem. Chem. Phys.*, 2017, **19**, 31306–31315.
29 R. N. Dsouza, U. Pischel and W. M. Nau, *Chem. Rev.*, 2011, **111**, 7941–7980.
30 M. Freitag, L. Gundlach, P. Piotrowiak and E. Galoppini, *J. Am. Chem. Soc.*, 2012, **134**, 3358–3366.
31 A. L. Koner and W. M. Nau, *Supramol. Chem.*, 2007, **19**, 55–66.
32 A. C. Bhasikuttan, J. Mohanty, W. M. Nau and H. Pal, *Angew. Chem. Int. Ed.*,

2007, **46**, 4120–4122.

33 F. C. Spano, *Acc. Chem. Res.*, 2010, **43**, 429–439.

34 S. Grimme, C. Bannwarth and P. Shushkov, *J. Chem. Theory Comput.*, 2017, **13**, 1989–2009.

35 K. I. Assaf, M. Florea, J. Antony, N. M. Henriksen, J. Yin, A. Hensen, Z.-w. Qu, R. Sure, D. Klapstein, M. K. Gilson, S. Grimme and W. M. Nau, *J. Phys. Chem. B*, 2017, **49**, 11144–11162.

36 S. Grimme and C. Bannwarth, *J. Chem. Phys.*, 2016, **145**, 054103.

37 S. Grimme, *J. Chem. Phys.*, 2013, **138**, 244104.